

# Coexistence of interdependence and competition in adaptive multilayer network

Nikita Frolov<sup>a,\*</sup>, Sarbendu Rakshit<sup>b</sup>, Vladimir Maksimenko<sup>a</sup>, Daniil Kirsanov<sup>a</sup>,  
Dibakar Ghosh<sup>b</sup>, Alexander Hramov<sup>a,\*</sup>

<sup>a</sup> Neuroscience and Cognitive Technology Laboratory, Center for Technologies in Robotics and Mechatronics Components, Innopolis University, Innopolis, 420500, The Republic of Tatarstan, Russia

<sup>b</sup> Physics and Applied Mathematics Unit, Indian Statistical Institute, 203 B. T. Road, Kolkata 700108, India

## ARTICLE INFO

### Article history:

Received 10 March 2021

Accepted 1 April 2021

### Keywords:

Explosive synchronization

Competition

Interdependence

Adaptive network

Multilayer network

## ABSTRACT

In dynamical networks, the presence of adaptation establishing the relationship between the coherence of local populations and unit's effective coupling provides the explosive transition – an abrupt transition from incoherence to coherence and vice versa through the hysteresis loop. Explosive transition is even possible under the coexistence of two opposite types of adaptation – interdependence and competition, wherein growing the competitive population dramatically narrows the area of hysteresis. Here, we demonstrate that considering a mixed adaptive model from a multilayer perspective expands the hysteresis region and shifts both forward and backward transition boundaries to the higher values of coupling strength as compared with a monolayer case. We show that this is due to greater robustness of the multilayer network against the intralayer topology and lower sensitivity to the amplification of the pre-bifurcation noise, i.e., spurious fluctuations of local coherence, in the vicinity of a tipping point as opposed to a single-layer network.

© 2021 Elsevier Ltd. All rights reserved.

## 1. Introduction

Onset and loss of synchronization in coupled oscillators are of fundamental importance in understanding several emergent behaviors in natural and artificial systems [1]. Synchronization of networked phase oscillators has proven itself to be an important process in understanding the collective behavior of a variety of real-world complex systems ranging from physical to biological systems [2].

The traditional route to coherence in complex networks implies a smooth growth/reduction of a synchronized cluster under the increase/decrease of the coupling between the interconnected units. On the opposite, explosive synchronization (ES) is the transition of an ensemble of networked oscillators from incoherence to coherence, which is first order, discontinuous and irreversible [3]. A central feature of such explosive transitions is the hysteresis behavior at the transition to synchronization. This emergent behavior was first reported in Ref. [4], and till now, it has been paid a great attention [5]. The discovery of such abrupt transitions has a vast

significance in real-world networks, including cascading failure of power grids [6], epileptic seizures in the brain [7], etc.

Explosive synchronization of complex networked oscillators was thought of as being rooted in the setting of specific microscopic correlation features between the natural frequency and the unit's degree in scale-free (SF) networks [8,9] or the natural frequencies of the oscillators and their effective coupling strengths [10–12]. This microscopic root in the setting of local correlation features was verified in the experimental setup of networked chaotic circuits with a star-like topology [13]. However, in Refs. [14,15], the authors show that ES occurs in adaptive single-layer and multilayer networks in the absence of such correlation properties. On the contrary, they establish the necessary condition for ES, which is a microscopic suppression (of any kind) of a global synchronization cluster. Later, M. Danziger et al. present a dynamic dependency framework that includes interdependence and competition rules for interaction between dynamical systems and facilitates various scenarios of explosive transitions [16].

Notably, the real networks do not always exhibit only cooperative or competitive types of adaptation, but it is likely that both mechanisms are presented in the network. For example, in cortical neural networks inhibitory (competitive) neurons coexist with excitatory (interdependent) ones, and their balance controls neuronal synchrony [17–19]. Several recent papers explore dynamical net-

\* Corresponding authors.

E-mail addresses: [n.frolov@innopolis.ru](mailto:n.frolov@innopolis.ru) (N. Frolov), [hramovae@gmail.com](mailto:hramovae@gmail.com) (A. Hramov).

works in the presence of attractive and repulsive coupling [20–22]. Moreover, X. Dai et al. [23] address the ES problem in populations of cooperative and competitive phase oscillators. They achieve that a relatively small fraction of competitor-units suppresses the hysteresis loop and switches the system to a continuous transition.

Besides, a growing literature evidences the constructive role of multiplex architecture to induce explosive transitions in the frequency-displaced [24], dissimilar [25], and phase-frustrated networks [26]. ES in multilayer networks is also yielded through the coupling of excitatory and inhibitory layers [27], time-delayed coupling [28], interlayer adaptation [29,30], and interlayer Hebbian plasticity [31]. It should be noteworthy that multilayer networks were the subject of close attention of Prof. Vadim S. Anishchenko and his team at Saratov State University. He has largely contributed to this field by the extensive analysis of coherence control via tuning interlayer couplings in multiplex networks [32–36].

In this work, we gather two opposite adaptive mechanisms in a multilayer configuration mainly to answer the following question: *How does multiplexing impacts ES in the network of coupled oscillators where interdependent and competitive interactions are simultaneously present?* We demonstrate that the additional layer shifts both forward and backward transition thresholds to the higher values of coupling strength as compared with a monolayer model. Moreover, a bilayer network exhibits hysteresis loop at larger population of competitive units. We find the explanation to the observed phenomenon in the difference between the forms of the adaptive terms in the monolayer and bilayer networks. These adaptive terms make the latter more robust against the spurious increases of local coherence in the vicinity of the tipping point and, thus, supports the discontinuity of the transition.

## 2. Mathematical model

We consider a bilayer ( $L = 2$ ) multiplex network having  $N$  Kuramoto phase oscillators in each layer (Fig. 1a) and compare its dynamics with a similar monolayer ( $L = 1$ ) network.

We begin a model description with a monolayer problem. Following Ref. [23], phase oscillators in a monolayer network with the mixing of interdependent and competitive units evolve in time as

$$\dot{\theta}_{i,1} = \omega_{i,1} + \lambda \mathcal{D}_i \sum_{j=1}^N \mathcal{A}_{ij} \sin(\theta_{j,1} - \theta_{i,1}), \quad (1)$$

where  $\theta_{i,1}$  and  $\omega_{i,1}$ ,  $i = 1, 2, \dots, N$  represent instantaneous phase and natural frequency of the  $i^{\text{th}}$  oscillator. The adjacency matrix  $\mathcal{A}$  encodes the underlying network architecture, where  $\mathcal{A}_{ij} = 1$ , if the nodes are connected, otherwise,  $\mathcal{A}_{ij} = 0$ , and  $\lambda$  depicts overall coupling strength. The degree of the  $i^{\text{th}}$  node is denoted by  $k_{i,1}$  and is defined as  $k_{i,1} = \sum_{j=1}^N \mathcal{A}_{ij}$ . We estimate spatial coherence of the local populations via complex local order parameter  $r_{i,1} \exp(i\Theta_{i,1}) = 1/k_{i,1} \sum_{j=1}^N \mathcal{A}_{ij} \exp(i\theta_{j,1})$ , such that  $r_{i,1} \in [0, 1]$  and  $\Theta_{i,1}$  being an average phase of the local population  $k_{i,1}$ .

The main feature of Eq. (1) is the presence of adaptive parameter  $\mathcal{D}_i$ . Being the function of the local order parameter,  $\mathcal{D}_i$  accounts for the nature of the dynamical dependence between the  $i^{\text{th}}$  unit and its neighbours. Since we consider coexistence of two adaptive mechanisms, we randomly choose a fraction of nodes  $f$  and adjust for all of them a competitive adaptation, which implies  $\mathcal{D}_i = 1 - r_{i,1}$ . The remaining fraction  $(1 - f)$  follows an interdependent rule, i.e.,  $\mathcal{D}_i = r_{i,1}$ .

Next, we introduce multiplexing by rewriting Eq. 1 in a bilayer fashion as

$$\begin{aligned} \dot{\theta}_{i,1} &= \omega_{i,1} + \lambda \mathcal{D}_i^{2 \rightarrow 1} \sum_{j=1}^N \mathcal{A}_{ij,1} \sin(\theta_{j,1} - \theta_{i,1}), \\ \dot{\theta}_{i,2} &= \omega_{i,2} + \lambda \mathcal{D}_i^{1 \rightarrow 2} \sum_{j=1}^N \mathcal{A}_{ij,2} \sin(\theta_{j,2} - \theta_{i,2}), \end{aligned} \quad (2)$$

(a) ● Competitive,  $fN$  ● Interdependent,  $(1-f)N$

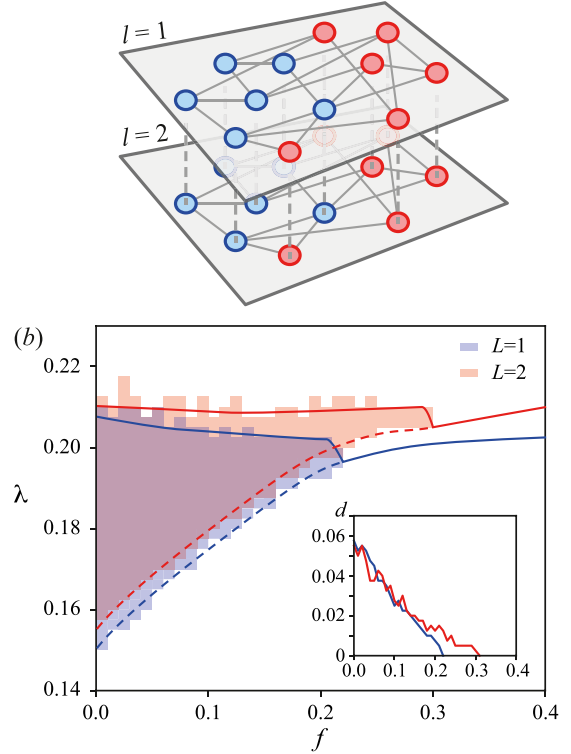


**Fig. 1.** (a) Illustration of a considered bilayer adaptive multiplex network with competitive (blue circles) and interdependent (red circles) units. Solid lines represent intralayer links encoded by adjacency matrix  $\mathcal{A}$  and dashed lines represent interlayer links between the replica nodes. (b) Hysteresis areas on the parameter plane ( $f, \lambda$ ) in the case of monolayer ( $L = 1$ , blue), and bilayer ( $L = 2$ , red) networks. Here, solid and dashed lines indicate approximate boundaries of forward and backward transitions. The inset reports the corresponding hysteresis width  $d$  versus  $f$  for mono- (blue line) and bilayer (red line) networks. (For interpretation of the references to color in this figure legend, the reader is referred to the web version of this article.)

where subscripts 1 and 2 correspond to layer-1 and its replica, layer-2, respectively. Notably, in a bilayer case,  $\mathcal{D}_i^{2 \rightarrow 1}$  and  $\mathcal{D}_i^{1 \rightarrow 2}$  define the nature of *interlayer* interaction, so that the adaptive parameter is controlled by the local order parameter of the *replica* unit from the opposite layer. In other words, for a competitive fraction  $f$  we define  $\mathcal{D}_i^{2 \rightarrow 1} = 1 - r_{i,2}$  and  $\mathcal{D}_i^{1 \rightarrow 2} = 1 - r_{i,1}$ , while for remaining (interdependent) fraction  $(1 - f)$  the adaptive rule is given by  $\mathcal{D}_i^{2 \rightarrow 1} = r_{i,2}$  and  $\mathcal{D}_i^{1 \rightarrow 2} = r_{i,1}$ . For simplicity of the analysis, we assume that the layers of considered multiplex network have the same architecture  $\mathcal{A}_{1,2} = \mathcal{A}$  and natural frequency distributions.

To evaluate macroscopic phase coherence of the network layers we use averaged global order parameter defined as

$$R_{1,2} = \frac{1}{N(t_{\max} - t_{tr})} \sum_{t=t_{tr}}^{t_{\max}} \left| \sum_{j=1}^N e^{i\theta_{j,\{1,2\}}(t)} \right|, \quad (3)$$

where  $t_{\max}$  and  $t_{tr}$  are maximal simulation time and duration of the transient period presented in the number of iterations.

In our numerical simulations [37] fully conducted in Julia programming language, we consider each layer as a random Erdős-Rényi (ER) network sized  $N = 10^3$  with mean degree  $\langle k \rangle_{\{1,2\}} = 1/N \sum_{i=1}^N k_{i,\{1,2\}} = 12$ . ER adjacency matrix is generated via MatrixDepot package. Natural frequencies  $\omega_{i,\{1,2\}}$  of interacting oscillators are drawn uniformly from the range  $[-1, 1]$ . Initial phases  $\theta_{i,\{1,2\}}$  are distributed homogeneously within the range  $[0, 2\pi)$ . We integrate Eqs. (1) and (2) numerically us-

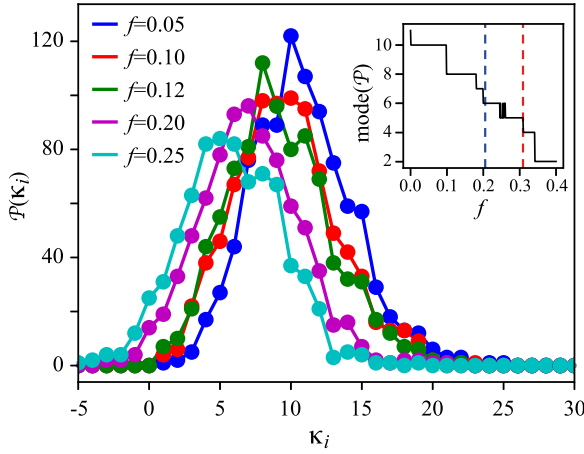


**Fig. 2.** Histograms  $\mathcal{P}(\kappa_i)$  over the interdependent units at different values of the competitive fraction size  $f$ . The inset illustrates the  $\text{mode}[\mathcal{P}(\kappa_i)]$  versus  $f$ . The critical values of  $f$  below which the mono- and bilayer networks exhibit ES according to Fig. 1b are shown in the inset with dashed vertical lines colored in blue and red, respectively. (For interpretation of the references to color in this figure legend, the reader is referred to the web version of this article.)

ing the 4-order Runge-Kutta (RK4) method implemented in the DifferentialEquations solver [38] with fixed time step  $dt = 10^{-2}$  time units, maximal simulation time  $t_{\max} = 1.5 \times 10^6$  iterations, and transient period  $t_{tr} = 1.2 \times 10^6$  iterations. To capture ES and associated hysteresis loop for each value of  $f$  we increased (decreased) overall coupling strength  $\lambda$  within the range  $[0.1, 0.25]$  with increment (decrement)  $\delta\lambda = 2.5 \times 10^{-3}$ .

### 3. Results

We find that in the adaptive network with coexisting competitive and interdependent units, multiplexing expands the area of hysteresis on the parameter plane  $(f, \lambda)$  compared with a monolayer case ( $L = 1$ ) as displayed by Fig. 1b. In a bilayer multiplex network, ES is observed for a larger size of a competitive population, and the forward transition boundary is shifted to higher values of the coupling strength  $\lambda$ . At the same time, the width of the hysteresis loop is approximately the same in both mono- and bilayer networks for  $f < 0.2$ . To access the impact of multiplexing on ES in this system we discuss the microscopic properties of individual nodes during the phase transitions in both mono- and bilayer networks.

Let us start the analysis by considering the topological properties of individual network nodes. As known from Refs. [14,23], the interdependent network fraction is vital for ES, and reduction of its population underlies transition to continuity by suppressing the hysteresis loop. Therefore, the nodes strongly connected with interdependent population are supposed to form a core group contributing to discontinuity. To measure node's coupling with the interdependent population we introduce the following quantity:

$$\kappa_i = \sum_{j \in \{1, 2, \dots, [fN]\}} \mathcal{A}_{ij} - \sum_{j \in \{[fN]+1, [fN]+2, \dots, N\}} \mathcal{A}_{ij}, \quad (4)$$

which implies for the  $i$ th unit the difference between the number of connections with interdependent and competitive populations. Fig. 2 shows the histograms  $\mathcal{P}(\kappa_i)$  over the interdependent nodes for different values of the competitive fraction size  $f$ . It is seen that with increasing  $f$  the histogram  $\mathcal{P}(\kappa_i)$  shifts to the lower values indicating that the number of links between the  $i$ th unit and the interdependent fraction nodes decreases with growing  $f$ . Notably, ES vanishes in the monolayer network as  $\text{mode}[\mathcal{P}(\kappa_i)] \leq \langle k \rangle / 2 = 6$  and in the bilayer network as  $\text{mode}[\mathcal{P}(\kappa_i)] \leq \langle k \rangle / 3 = 4$ . We conclude from the above that the bilayer multiplex network is more

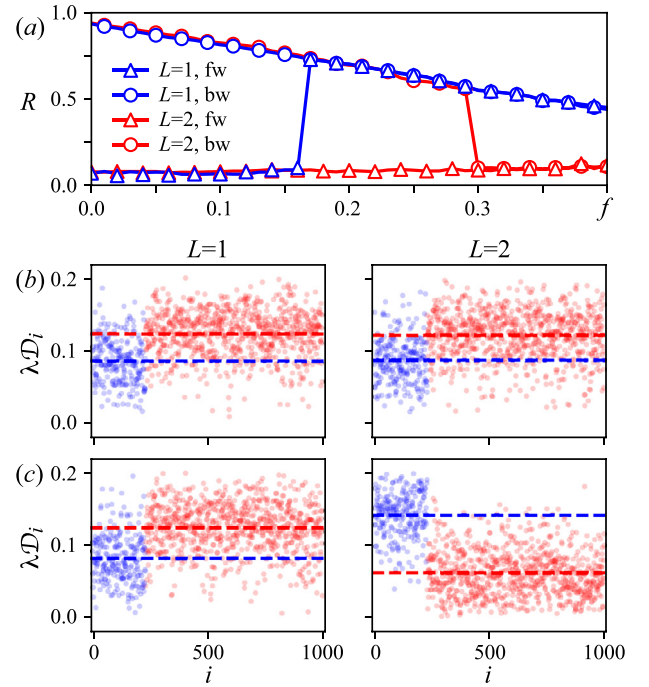


**Fig. 3.** Bilayer network versus Monolayer network. (a) Slices of forward (fw, triangles) and backward (bw, circles) transitions versus the competition fraction size  $f$  in bilayer (red) and monolayer (blue) networks for  $\lambda = 0.205$ . Scatterplots (b)-(c) report the effective coupling  $\lambda \mathcal{D}_i$  at  $t = t_{\max}$  versus the unit's index for monolayer (left column) and bilayer (right column) networks during backward (b) and forward (c) transitions for  $f = 0.23$  and  $\lambda = 0.205$ . Here, interdependent and competitive nodes are presented by red and blue dots, respectively. (For interpretation of the references to color in this figure legend, the reader is referred to the web version of this article.)

robust to the loss of connectivity within the interdependent fraction as opposed to the monolayer model.

We now proceed by explicitly considering the relation between macroscopic network state and microscopic properties of individual units. We are mainly interested in the area of the parameter plane  $(f, \lambda)$  where a bilayer network exhibits larger hysteresis region. Fig. 3a reports the changes in macroscopic network states of the mono- and bilayer models under the variation of  $f$  at fixed  $\lambda = 0.205$  during forward and backward transitions. One can see that in the monolayer network ES is suppressed as competitive fraction size  $f$  exceeds a critical value of 0.16. For  $f > 0.16$ , a monolayer model converges to a partially coherent state during both forward and backward transitions. A bilayer network, in turn, facilitates coherent state at larger size of the competitive population up to  $f = 0.3$ . Then the bilayer network exhibits turbulent behaviour abruptly. However, for the backward transitions it remains in incoherent state. To draw the difference between the mono- and bilayer models we focus our attention on the area  $0.16 < f < 0.3$  and for definiteness fix  $f = 0.23$ . Fig. 3b and c present the effective coupling strength  $\lambda \mathcal{D}_i$  versus the unit's index in the monolayer network (left) and layer-1 of the bilayer network (right) for backward and forward transitions, respectively. As seen from Fig. 3b, during the backward transition both models demonstrate similar distribution of  $\lambda \mathcal{D}_i$ : the fraction of interdependent units (red dots) dominates over the competitive ones (blue dots) due to higher values of effective coupling. In turn, different behaviors are observed in the case of forward transition (Fig. 3c). While the monolayer network remains partially coherent in terms of macroscopic state with the dominance of interdependent population, the opposite situation is observed in a bilayer model, where macroscopic incoherence is supported by a strongly coupled competitive fraction.

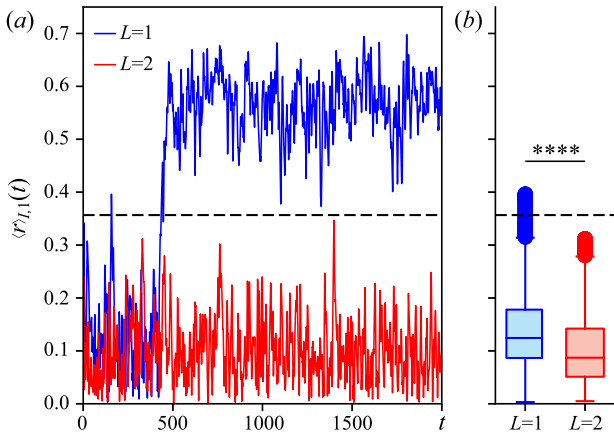


**Fig. 4.** (a) Time-series of order parameter averaged over the interdependent population  $\langle r \rangle_{l,1}(t)$  of the monolayer network (blue) and layer-1 of the bilayer network (red) for  $f = 0.23$  and  $\lambda = 0.205$ . Black dashed line indicates the 99th percentile of  $R$  in the monolayer network before the transition to coherence, i.e., at the time interval 0–400 time units. (b) Boxplots of global order parameter values at the time interval 0–400 time units in the monolayer network (blue) and layer-1 of the bilayer network (red). Here, “\*\*\*\*” reports the significance level of  $p < 0.0001$  via unpaired  $t$ -test. (For interpretation of the references to color in this figure legend, the reader is referred to the web version of this article.)

Thus, we conclude that adaptation *through the multiplexing* contributes greater to the suppression of coherence in the interdependent population. Therefore, it provides an ES-associated hysteresis loop in the bilayer network in those conditions in which it is not observed in a monolayer case.

We extend our understanding of the effect of multiplexing by considering corresponding time-series of the averaged local order parameter over the interdependent population in the monolayer network and layer-1 of the bilayer model defined as

$$\langle r \rangle_{l,1}(t) = \frac{1}{(1-f)N} \sum_{j \in \{\lceil fN \rceil + 1, \lceil fN \rceil + 2, \dots, N\}} r_{j,1}(t).$$

Fig. 4a shows that the interdependent population of monolayer network undergoes an abrupt transition to coherence at approximately 400 time units, while the same group in the layer-1 of bilayer network remains long-term incoherent. As both networks at  $\lambda = 0.205$  and  $f = 0.23$  are in the vicinity of a tipping point, they exhibit a pre-bifurcation noise amplification [39], or fluctuations of local coherence  $\langle r \rangle_{l,1}$ . At the same time, as displayed by Fig. 4b, the level of  $\langle r \rangle_{l,1}$  preceding the transition is significantly higher in the monolayer network than in the layer-1 of the bilayer network over the same time period. Also, the number of outliers in  $\langle r \rangle_{l,1}$  distribution, or rare random events of local coherence increase, is larger in the monolayer network as compared with the bilayer model. Notably, a globally coherent state is developed from one of such events. Based on the above, we suggest that the adaptation mechanism in a monolayer network contributes greater to amplifying such random short-term fluctuations of coherence as opposed to a bilayer model.

Indeed, taking into account the complex form of local order parameter  $r_{i,1} \exp(i\Theta_1) = 1/k_{i,1} \sum_{j=1}^N A_{ij} \exp(i\theta_{j,1})$  and rewriting Eq. (1) for the interdependent units in a monolayer network, we obtain:

$$\dot{\theta}_{i,1} = \omega_{i,1} + \lambda k_{i,1} r_{i,1}^2 \sin(\Theta_1 - \theta_{i,1}). \quad (5)$$

Repeating the same procedure for the interdependent units in a bilayer model we obtain:

$$\begin{aligned} \dot{\theta}_{i,1} &= \omega_{i,1} + \lambda k_{i,2} r_{i,1} r_{i,2} \sin(\Theta_1 - \theta_{i,1}), \\ \dot{\theta}_{i,2} &= \omega_{i,2} + \lambda k_{i,1} r_{i,1} r_{i,2} \sin(\Theta_2 - \theta_{i,2}). \end{aligned} \quad (6)$$

It follows from Eq. (5) that in a rewritten form an effective coupling term for a monolayer model is proportional to a squared local order parameter of the current layer  $r_{i,1}^2$ . It implies that sufficiently large spurious fluctuations of local coherence would self-consistently boost their growth through the increase of the unit's effective coupling term. In turn, as seen from Eq. (6), an effective coupling term in a bilayer network depends on the product of local order parameters on the current and the opposite layers  $r_{i,1} r_{i,2}$ . In this case, the gain of effective coupling is possible only under the simultaneous increase of the local coherence in both current population and its replica on the opposite layer. It means that such form of interdependence between the layers is less sensitive to the random fluctuations of local coherence as compared with a monolayer model. Thus, we conclude that precisely the mutual dependence between the layer in a multiplex model forces the maintaining of incoherence and by this supports discontinuity in a wider range of system's control parameters as opposed to a monolayer case.

#### 4. Conclusion

As reported in the previous papers [14,15], the presence of any factor suppressing the formation of a large coherent cluster provides the conditions for ES in complex networks. Specifically, the interdependent adaptive rule, i.e., the relationship between effective coupling and local order parameter, is proven to be one of them. Further, it has been shown that explosive transition may be found even under mixing of two opposite adaptive mechanisms – interdependence and competition – within a complex network [23]. Here, we evidence that multilayer architecture expands the area of hysteresis associated with ES in such mixed adaptive models. First, we obtain that the suppression of ES in the mixed adaptive model is related to the loss of the connectivity within an interdependent fraction, which is a core population supporting discontinuity, and the multilayer network is more robust against this factor as compared with a monolayer one. Second, we achieve the shift of ES thresholds to the higher values of coupling strength and maintenance of hysteresis at a larger size of competitive fraction in the multilayer network. We establish that this is due to a higher sensitivity of a monolayer network to a pre-bifurcation noise amplification in the vicinity of a tipping point as compared to a multilayer case.

A considered model with coexisting interdependent and competitive mechanisms of adaptation has a certain degree of similarity with real networks. For instance, the local neuronal population of the brain cortex is known to be comprised of excitatory (cooperative) and inhibitory (competitive) neurons [17–19]. Despite a small proportion, the inhibitory neurons are vital in the regulation of neuronal coherence. We expect that our results may be of a certain value in understanding the properties of activation in neuronal ensembles under the influence of factors varying the inhibition level.

#### Declaration of Competing Interest

The authors declare that they have no known competing financial interests or personal relationships that could have appeared to influence the work reported in this paper.

#### CRedit authorship contribution statement

**Nikita Frolov:** Conceptualization, Methodology, Software, Formal analysis, Funding acquisition, Supervision, Visualization, Writing - original draft, Writing - review & editing. **Sarbendu Rakshit:** Software, Formal analysis, Writing - original draft. **Vladimir Maksimenko:** Conceptualization, Writing - original draft. **Daniil Kirsanov:** Software. **Dibakar Ghosh:** Methodology, Funding acquisition.



tion, Supervision, Writing - review & editing. **Alexander Hramov:** Conceptualization, Funding acquisition, Writing - review & editing.

## Acknowledgments

This work was supported by the [Russian Foundation for Basic Research](#) (Grant no. 19-52-45026) and the Department of Science and Technology, Government of India (Project no. INT/RUS/RFBR/360 ). A.E.H. acknowledges the President Program of Leading Russian Scientific School Support (Grant no. NSH-2594.2020.2).

## References

- [1] Pikovsky A, Kurths J, Rosenblum M, Kurths J. Synchronization: a universal concept in nonlinear sciences. Cambridge university press; 2003.
- [2] Arenas A, Díaz -Guilera A, Kurths J, Moreno Y, Zhou C. Synchronization in complex networks. *Phys Rep* 2008;469(3):93–153.
- [3] Boccaletti S, Almendral J, Guan S, Leyva I, Liu Z, Sendina Nadal I, Wang Z, Zou Y. Explosive transitions in complex networks structure and dynamics: Percolation and synchronization. *Phys Rep* 2016;660:1–94.
- [4] Pazó D. Thermodynamic limit of the first-order phase transition in the Kuramoto model. *Phys Rev E* 2005;72(4):046211.
- [5] Călugăru D, Totz JF, Martens EA, Engel H. First-order synchronization transition in a large population of strongly coupled relaxation oscillators. *Sci Adv* 2020;6(39):eabb2637.
- [6] Buldyrev SV, Parshani R, Paul G, Stanley HE, Havlin S. Catastrophic cascade of failures in interdependent networks. *Nature* 2010;464(7291):1025–8.
- [7] Wang Z, Tian C, Dhamala M, Liu Z. A small change in neuronal network topology can induce explosive synchronization transition and activity propagation in the entire network. *Sci Rep* 2017;7(1):1–10.
- [8] Gómez-Gardeñes J, Gómez S, Arenas A, Moreno Y. Explosive synchronization transitions in scale-free networks. *Phys Rev Lett* 2011;106(12):128701.
- [9] Liu W, Wu Y, Xiao J, Zhan M. Effects of frequency-degree correlation on synchronization transition in scale-free networks. *EPL (Europhys Lett)* 2013;101(3):38002.
- [10] Zhang X, Hu X, Kurths J, Liu Z. Explosive synchronization in a general complex network. *Phys Rev E* 2013;88(1):010802.
- [11] Leyva I, Sendina-Nadal I, Almendral J, Navas A, Olmi S, Boccaletti S. Explosive synchronization in weighted complex networks. *Phys Rev E* 2013;88(4):042808.
- [12] Leyva I, Navas A, Sendina-Nadal I, Almendral J, Buldú J, Zanin M, Papo D, Boccaletti S. Explosive transitions to synchronization in networks of phase oscillators. *Sci Rep* 2013;3(1):1–5.
- [13] Leyva I, Sevilla-Escoboza R, Buldú J, Sendina-Nadal I, Gómez-Gardeñes J, Arenas A, Moreno Y, Gómez S, Jaimes-Reátegui R, Boccaletti S. Explosive first-order transition to synchrony in networked chaotic oscillators. *Phys Rev Lett* 2012;108(16):168702.
- [14] Zhang X, Boccaletti S, Guan S, Liu Z. Explosive synchronization in adaptive and multilayer networks. *Phys Rev Lett* 2015;114(3):038701.
- [15] Danziger MM, Moskalenko OI, Kurkin SA, Zhang X, Havlin S, Boccaletti S. Explosive synchronization coexists with classical synchronization in the kuramoto model. *Chaos* 2016;26(6):065307.
- [16] Danziger MM, Bonamassa I, Boccaletti S, Havlin S. Dynamic interdependence and competition in multilayer networks. *Nat Phys* 2019;15(2):178–85.
- [17] Marín-Burgin A, Mongiat LA, Pardi MB, Schinder AF. Unique processing during a period of high excitation/inhibition balance in adult-born neurons. *Science* 2012;335(6073):1238–42.
- [18] Xue M, Atallah BV, Scanziani M. Equalizing excitation–inhibition ratios across visual cortical neurons. *Nature* 2014;511(7511):596–600.
- [19] Okun M, Lampl I. Instantaneous correlation of excitation and inhibition during ongoing and sensory-evoked activities. *Nat Neurosci* 2008;11(5):535–7.
- [20] Frolov N, Maksimenko V, Majhi S, Rakshit S, Ghosh D, Hramov A. Chimera-like behavior in a heterogeneous Kuramoto model: The interplay between attractive and repulsive coupling chaos: an interdisciplinary. *J Nonlinear Sci* 2020;30(8):081102.
- [21] Majhi S, Chowdhury SN, Ghosh D. Perspective on attractive–repulsive interactions in dynamical networks: progress and future. *EPL (Europhys Lett)* 2020;132(2):20001.
- [22] Chowdhury SN, Ghosh D, Hens C. Effect of repulsive links on frustration in attractively coupled networks. *Phys Rev E* 2020;101(2):022310.
- [23] Dai X, Li X, Gutiérrez R, Guo H, Jia D, Perc M, Manshour P, Wang Z, Boccaletti S. Explosive synchronization in populations of cooperative and competitive oscillators. *Chaos Solitons Fractals* 2020;132:109589.
- [24] Jalan S, Kumar A, Leyva I. Explosive synchronization in frequency displaced multiplex networks. *Chaos* 2019;29(4):041102.
- [25] Jalan S, Kachhvah AD, Jeong H. Explosive synchronization in multilayer dynamically dissimilar networks. *J Comput Sci* 2020;46:101177.
- [26] Khanra P, Kundu P, Hens C, Pal P. Explosive synchronization in phase-frustrated multiplex networks. *Phys Rev E* 2018;98(5):052315.
- [27] Jalan S, Rathore V, Kachhvah AD, Yadav A. Inhibition-induced explosive synchronization in multiplex networks. *Phys Rev E* 2019;99(6):062305.
- [28] Kachhvah AD, Jalan S. Delay regulated explosive synchronization in multiplex networks. *New J Phys* 2019;21(1):015006.
- [29] Kumar A, Jalan S, Kachhvah AD. Interlayer adaptation-induced explosive synchronization in multiplex networks. *Phys Rev Res* 2020;2(2):023259.
- [30] Pitsik E, et al. Inter-layer competition in adaptive multiplex network. *New J Phys* 2018;20(7):075004. doi:10.1088/1367-2630/aad00d.
- [31] Kachhvah AD, Dai X, Boccaletti S, Jalan S. Interlayer Hebbian plasticity induces first-order transition in multiplex networks. *New J Phys* 2020;22(12):122001.
- [32] Shepelev I, Bukh A, Strelkova G, Anishchenko V. Anti-phase relay synchronization of wave structures in a heterogeneous multiplex network of 2D lattices. *Chaos Solitons Fractals* 2021;143:110545.
- [33] Rybalova E, Strelkova G, Anishchenko V. Impact of sparse inter-layer coupling on the dynamics of a heterogeneous multilayer network of chaotic maps. *Chaos Solitons Fractals* 2021;142:110477.
- [34] Rybalova E, Strelkova G, Schöll E, Anishchenko V. Relay and complete synchronization in heterogeneous multiplex networks of chaotic maps. *Chaos* 2020;30(6):061104.
- [35] Winkler M, Sawicki J, Omelchenko I, Zakharova A, Anishchenko V, Schöll E. Relay synchronization in multiplex networks of discrete maps. *EPL (Europhys Lett)* 2019;126(5):50004.
- [36] Rybalova E, Vadivasova T, Strelkova G, Anishchenko VS, Zakharova A. Forced synchronization of a multilayer heterogeneous network of chaotic maps in the chimera state mode. *Chaos* 2019;29(3):033134.
- [37] Simulation code is available online at <https://github.com/nikfrlv/jukunet-mad.git>.
- [38] Rackauckas C, Nie Q. Differentialequations. jl—a performant and feature-rich ecosystem for solving differential equations in julia. *J Open Res Softw* 2017;5(1):15.
- [39] Surovyatkina E, Kravtsov YA, Kurths J. Fluctuation growth and saturation in nonlinear oscillators on the threshold of bifurcation of spontaneous symmetry breaking. *Phys Rev E* 2005;72(4):046125.